PHYSICAL REVIEW B **77**, 104111 (2008)

Infrared and magnetic characterization of multiferroic Bi_2FeCrO_6 thin films over a broad temperature range

S. Kamba,[1,*] D. Nuzhnyy,[1] R. Nechache,[2] K. Závěta,[3] D. Nižňanský,[4] E. Šantavá,[1] C. Harnagea,[2] and A. Pignolet[2]
[1]*Institute of Physics ASCR, Na Slovance 2, 182 21 Prague 8, Czech Republic*
[2]*INRS-Énergie, Materiaux et Télécommunications, 1650 Boulevard Lionel-Boulet, Varennes, Quebec, Canada, J3X 1S2*
[3]*Faculty of Mathematics and Physics, Charles University, V Holešovičkách 2, 18000 Prague 8, Czech Republic*
[4]*Faculty of Natural Sciences, Charles University, Albertov 6, 128 43 Prague 2, Czech Republic*
and Institute of Inorganic Chemistry, ASCR, 250 68 Rez near Prague, Czech Republic

(Received 6 December 2007; revised manuscript received 5 February 2008; published 12 March 2008)

Infrared reflectance spectra of an epitaxial Bi_2FeCrO_6 thin film prepared by pulsed laser deposition on $LaAlO_3$ substrate were recorded between 10 and 900 K. No evidence for a phase transition to the paraelectric phase was observed, but some phonon anomalies were revealed near 600 K. Most of the polar modes exhibit only a gradual softening, which results in a continuous increase of the static permittivity on heating. It indicates that the phase transition from ferroelectric to paraelectric phase should occur somewhere above 900 K. Magnetic measurements of the partially *B*-site-ordered Bi_2FeCrO_6 thin film deposited on Nb-doped $SrTiO_3$ substrate were performed up to 1000 K. They revealed a possible magnetic phase transition between 600 and 800 K, but the exact critical temperature cannot be determined due to a strong diamagnetic signal from the substrate. Nevertheless, our experimental data show that the *B*-site-ordered Bi_2FeCrO_6 is one of the rare high-temperature multiferroics.

DOI: 10.1103/PhysRevB.77.104111 PACS number(s): 77.22.−d, 78.30.−j, 74.25.Ha, 63.20.−e

I. INTRODUCTION

Magnetoelectric multiferroic materials which exhibit simultaneously ferroelectric and magnetic order are promising for new generation of random access memories (RAMs), where the information can be written by electric field and read nondestructively by magnetic sensing. Such memories avoid the weak points of the ferroelectric RAMs (destructive reading causes fatigue) as well as of magnetic RAMs (high electric current is needed for overwriting, which rules out high integration of magnetic RAMs). Unfortunately, there are not many magnetoelectric single phase multiferroics known up to now and only a few of them have both magnetic and ferroelectric critical temperatures above room temperature. Therefore, there is, nowadays, an intensive search for magnetoelectric multiferroic materials with high magnetization and spontaneous polarization above room temperature.[1,2]

Baettig and Spaldin predicted from *ab initio* calculations that the chemically ordered double perovskite Bi_2FeCrO_6 (BFCO) will have—at zero temperature—a polarization of $\sim 80\ \mu C/cm^2$ and a magnetization of $\sim 160\ emu/cm^3$ ($2\mu_B$/f.u.).[3] Such properties far exceed the properties of any known multiferroic. Nechache *et al.*, for the first time, experimentally prepared an epitaxial thin film of BFCO which exhibited at room temperature (RT) a polarization of $2.8\ \mu C/cm^2$ and a saturated magnetization of $0.26\mu_B$ per unit cell.[4,5] Recently, Kim *et al.*[6] reported a remanent polarization of $60\ \mu C/cm^2$ at 77 K for their $BiFe_{0.5}Cr_{0.5}O_3$ solid solution epitaxial films and Alexe even measured $70-80\ \mu C/cm^2$ at RT on the films grown by Nechache *et al.*[7] The magnetic T_N and ferroelectric T_c phase transition temperatures in ordered BFCO are not known up to now. Beattig *et al.*[8] predicted from first principles a Néel temperature T_N near 100 K, which was not confirmed in the experiments performed by Nechache *et al.*, who observed magnetic order at RT. Very recently, Suchomel *et al.*[9] prepared BFCO ceramics and observed a magnetic phase transition below 130 K, but it is worth noting that their ceramics exhibited chemical disorder of the Fe^{3+} and Cr^{3+} cations on the perovskite *B* site, which reduces T_N. Thus, it is not excluded that T_N can be higher in ordered samples as in the case for the ordered BFCO films reported by Nechache *et al.*[10]

Determination of the ferroelectric phase transition temperature is not possible from the low-frequency dielectric measurements due to the too high dc conductivity of the BFCO film. The extrinsic leakage conductivity does not play an appreciable role in the terahertz dielectric response of the film; therefore, high-frequency dielectric studies are advantageous. For this purpose, we performed infrared (IR) measurements including investigation in hardly achievable far infrared (FIR) range below $200\ cm^{-1}$, which can give information about the complete phonon contributions to the static permittivity (note that in the case of displacive ferroelectrics, only polar phonons are responsible for the dielectric anomaly near T_c). Moreover, IR spectra usually change at the ferroelectric (structural) phase transition temperature due to the change of selection rules for IR active polar phonons. Therefore, the IR spectra (including FIR) of the BFCO film can help to estimate its T_c as well as the symmetry of the high-temperature phase.

IR studies of ferroelectric thin films are rather rare in the literature and, up to now, almost only FIR transmission spectra of the films deposited on FIR-transparent substrates such as Si, sapphire, or MgO were investigated. FIR transmission can give results only in a limited frequency range determined by the transparency window of the substrates, which is mostly very narrow, particularly at high temperatures (e.g., sapphire is partially transparent only below $150\ cm^{-1}$ at 900 K).[11] IR reflectance can yield results in a much broader

©2008 The American Physical Society

spectral range, but its sensitivity is limited (a) by the thickness of the film, (b) by the strengths of polar phonons in the IR spectra, and (c) by the IR properties of the substrate. Our experience shows that the substrates with buffer electrodes are not suitable due to the negative permittivity of the buffer layers, which reduces the sensitivity of the method. Therefore, dielectric substrates, which do not show any strongly temperature-dependent IR reflectivity spectra, are the most suitable for reflectance studies of thin films. Nevertheless, IR reflectance spectra of the thin films deposited on the substrate are strongly influenced by the substrate since the thin films are partially transparent for the IR wavelength. Therefore, both IR spectra of the bare substrate and of the film on the substrate should be measured at the same temperatures, and the film properties are evaluated from the spectra fits to such a multilayer system. This method was used only twice in the literature for room or low-temperature IR studies of $SrTiO_3$ films.[12,13] Here, we will use this method above room temperature and even up to 900 K.

In this paper, we shall show that the static permittivity of the BFCO thin film, determined from the polar phonon contributions, increases monotonically on heating to 900 K, due to the phonon softening. Some phonon anomalies, probably connected with a magnetic phase transition, were observed near 600 K, but no dramatic changes, such as those usually related to a ferroelectric phase transition, were observed. Therefore, it seems that the phase transition to the paraelectric phase in BFCO thin film occurs above the highest investigated temperature of 900 K. We shall also report on our study the magnetic properties of the BFCO films up to 1000 K and we shall show that the magnetic phase transition occurs between 600 and 800 K.

II. EXPERIMENT

BFCO films were grown directly on (100)-oriented $SrTiO_3$ substrates doped with 0.5 wt % of Nb (abbreviated STO:Nb) as well as on a (100)-oriented $LaAlO_3$ substrate, better suited for IR measurements. An epitaxial 210 nm thick film deposited on the conducting STO:Nb substrate was used for Mössbauer spectroscopy and vibrating-sample magnetometry studies. X-ray diffraction (XRD) and transmission electron microscopy (TEM) data have shown that the thin film is epitaxial. Superlattice spots showed evidence of partial chemical order of the Fe and Cr cations.[10]

The $SrTiO_3$ substrate exhibits a strongly temperature-dependent FIR spectra due to the presence of an optic soft mode, which gives large inaccuracies in the evaluation of the FIR properties of the thin film. We therefore studied FIR spectra of the BFCO film deposited on nonconducting $LaAlO_3$ substrates with the size of $5\times10\times0.5$ mm^3. Since polar phonons are rather weak in BFCO, we investigated a 600 nm thick film. The relaxed film on $LaAlO_3$ substrate was epitaxial with orientation (001), but it revealed only very weak superlattice spots, so its chemical order in the B site was only partial. XRD analysis of the film on $LaAlO_3$ revealed a slight Bi deficiency in the BFCO phase as well as about 5% of Cr-doped Bi_2O_3 secondary phase, which were not observed for the films on $SrTiO_3$.

The unpolarized FIR and IR reflectance spectra were taken using a Bruker IFS 113v Fourier transform IR spectrometer at temperatures between 10 and 900 K with the resolution of 2 cm^{-1}. An optistat continuous flow cryostat from Oxford Instruments equipped with polyethylene windows was used for cooling the sample down to 10 K, while a commercial high-temperature cell Specac P/N 5850 was used for heating it up to 900 K. A helium-cooled Si bolometer operating at 1.6 K was used as a detector at low-temperature measurements, while pyroelectric DTGS detectors were used for the IR measurements above RT.

Magnetic properties of the BFCO films on substrates 3×3 mm^2 in size were investigated using a PPMS 14 vibrating-sample magnetometer (Quantum Design) between 3 and 1000 K. Magnetization was measured in two orientations, $B\parallel(001)$ and $B\perp$ (001) planes.

The Mössbauer spectrum measurement was carried out in the conversion electron Mössbauer spectroscopy (CEMS) mode with ^{57}Co diffused into an Rh matrix as a source moving with a constant acceleration. The spectrum was accumulated for 7 days. Classical Mössbauer spectroscopy in transmission mode could not be used due to the small volume of the investigated thin films. The Wissel spectrometer was calibrated by means of a standard α-Fe foil, and the isomer shift was expressed with respect to this standard at 293 K. The fitting of the spectra was performed using the NORMOS program. The CEMS method requires a conducting sample; therefore, we investigated the thin film deposited on a conducting STO:Nb substrate, while the films deposited on nonconducting $LaAlO_3$ were more suitable for the IR studies.

III. RESULTS AND DISCUSSION

Figure 1 shows IR reflectance spectra of both a pure $LaAlO_3$ substrate and a BFCO thin film (deposited on $LaAlO_3$) at selected temperatures between 10 and 900 K. Only small temperature dependence of the reflectivity spectra of the $LaAlO_3$ substrate can be seen, mostly due to an increase in phonon damping with temperature. Also, the sharp peaks near 500 and 600 cm^{-1} gradually disappear due to a second order structural phase transition in $LaAlO_3$ from trigonal to cubic phase at 800 K.[14]

IR reflectance spectra of the semitransparent BFCO film deposited on the opaque $LaAlO_3$ substrate exhibits more pronounced changes with temperature mainly near 100, 250, and 550 cm^{-1} (marked by arrows in Fig. 1). For the detailed analysis, we evaluated the complex permittivity $\varepsilon^*(\omega)=\varepsilon'(\omega)-i\varepsilon''(\omega)$ spectra of the film (see Fig. 2) using the following procedure: the reflectivity $R(\omega)$ of the bare substrate at each temperature was first fitted using the formula

$$R(\omega)=\left|\frac{\sqrt{\varepsilon^*(\omega)}-1}{\sqrt{\varepsilon^*(\omega)}+1}\right|^2, \tag{1}$$

where for $\varepsilon^*(\omega)$ the factorized form of the complex permittivity[15] was used,

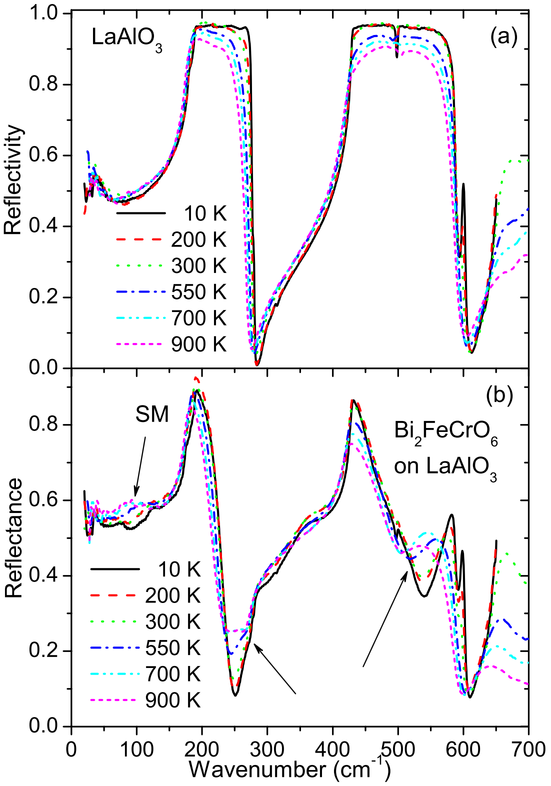

FIG. 1. (Color online) (a) Infrared reflectivity spectra of LaAlO$_3$ substrate and (b) reflectance spectra of Bi$_2$FeCrO$_6$ film (600 nm thick) deposited on LaAlO$_3$. The arrows show anomalous phonons. Note that 1 cm^{-1} corresponds to 30 GHz.

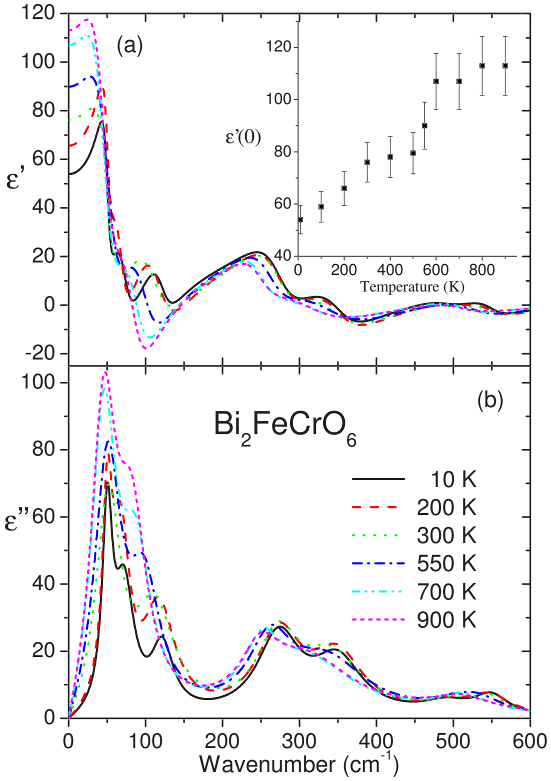

FIG. 2. (Color online) Complex dielectric spectra of the BFCO film obtained at selected temperatures from the fit of the reflectance spectra in Fig. 1. Frequencies of the peaks in $\varepsilon''(\omega)$ spectra roughly correspond to the TO phonon frequencies. Note the continuous increase of the static permittivity $\varepsilon'(0)$ with rising temperature (see inset).

$$\varepsilon^*(\omega) = \varepsilon_\infty \prod_j \frac{\omega_{LOj}^2 - \omega^2 + i\omega\gamma_{LOj}}{\omega_{TOj}^2 - \omega^2 + i\omega\gamma_{TOj}}. \qquad (2)$$

ω_{TOj} and ω_{LOj} denote the frequencies of the jth transverse and longitudinal polar phonons, respectively, and γ_{TOj} and γ_{LOj} denote their corresponding damping constants. The high-frequency permittivity ε_∞ results from the electron absorption processes and from the phonon contribution above 600 cm^{-1}. Then, the spectrum of the two-slab system (film + substrate) was fitted using the full formula for the coherent reflectance of a two-layer system,[16,17] where the oscillator parameters of the substrate were fixed, in order to determine the oscillator parameters of the polar phonons in the film. We note that for the film IR spectra fits, we used the classical Lorentz model of the damped harmonic oscillators instead of Eq. (2),

$$\varepsilon^*(\omega) = \varepsilon_\infty + \sum_{j=1}^{n} \frac{\Delta\varepsilon_j \omega_{TOj}^2}{\omega_{TOj}^2 - \omega^2 + i\omega\gamma_{TOj}}, \qquad (3)$$

where $\Delta\varepsilon_j$ means the contribution of the jth mode to the static permittivity. The rest of the parameters in Eq. (3) have the same meaning as in Eq. (2). Equation (2) is more suitable for the reflectivity fits of phonon spectra with a large TO-LO splitting, when both kinds of phonon modes have different damping. Such a model was necessary to use for a good fit of the LaAlO$_3$ substrate. Equation (3) is more appropriate for fitting of the reflectivity spectra of phonons with a small TO-LO splitting and/or transmission spectra which do not show up anomalies at LO frequencies. It has fewer parameters and gives acceptable physical results, while the former model can sometimes yield unphysical negative dielectric losses, when the parameters are not properly chosen.

Complex dielectric spectra of BFCO film obtained from the above described fit of the IR reflectance spectra displayed in Fig. 1 are plotted in Fig. 2. The temperature dependence of TO phonon frequencies is plotted in Fig. 3. One can clearly see the shift of most of the phonon modes to lower frequencies on heating (phonon softening). It causes the gradual increase of the static permittivity with rising temperature (see inset in Fig. 2).

Six modes (seven below 200 K) were necessary for the fits. Let us compare the number of observed polar modes with the prediction of factor group analysis. Bulk BFCO crystallizes at room temperature in the rhombohedral space group $R3-C_3^4$.[3,8] LaAlO$_3$ substrate has a much smaller lattice constant (3.79 Å) than bulk BFCO (3.932);[6] therefore, the thin film should be compressively stressed and should exhibit a tetragonal structure. However, the misfit between the substrate and BFCO is too large (3.7%); therefore, the strain relaxes in our 600 nm thick BFCO film and its structure again becomes rhombohedral like in the bulk.

In Table I, we present the factor group analysis (i.e., symmetries and activities in IR and Raman spectra) of the optic

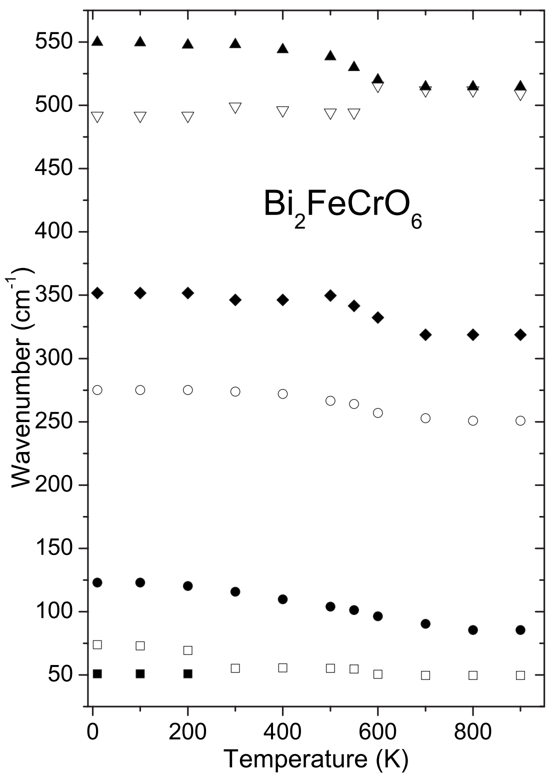

FIG. 3. Temperature dependence of the transverse polar phonon eigenfrequencies in the BFCO film deposited on LaAlO$_3$.

lattice vibrations in ferroelectric rhombohedral structure as well as in various possible higher-temperature phases. The analysis was performed using the tables published by Rousseau *et al.*[18] Here, we assume that BFCO has a similar sequence of phases at high temperatures as BiFeO$_3$. Recently, it was assumed that BiFeO$_3$ undergoes only one structural (and ferroelectric) phase transition near 1120 K to cubic $Pm\bar{3}m$ phase. However, new structural studies[19] revealed an intermediate orthorhombic phase with the space group C_{2v}^1-$P2mm$ or C_{2v}^{11}-$C2mm$ at temperatures between ~1100 and ~1200 K and probably only above ~1200 K BiFeO$_3$ transforms into the cubic and simultaneously conducting phase.[19] Kornev*et al.*[20] recently predicted a tetragonal intermediate phase $I4/mcm$-D_{4h}^{18} from *ab initio* calculations but, finally, their crystal structure refinement (performed on powder) revealed a monoclinic structure with space group $C2/m$-C_{2h}^3. Both phases should be nonpolar.

Our epitaxial BFCO film is (001) oriented and since we measure the in-plane response, we see mostly the E symmetry modes in our FIR spectra. We resolved seven modes in the low-temperature spectra, although nine E modes are allowed. This is quite reasonable, if we take into account that some of the modes have small intensity or they may overlap with other modes. It is worth noting that the TO phonon frequencies in BFCO correspond very well to the E symmetry TO phonon frequencies in chemically and structurally related BiFeO$_3$.[21–23]

One mode near 50 cm^{-1} disappears from the FIR spectra above 200 K (see black solid squares in Fig. 3). Such change could be a hint of some structural phase transition, but the FIR spectra near 50 cm^{-1} are rather noisy at high temperatures, so we cannot exclude that the mode is present in the spectra also at higher temperatures, but we do not resolve it due to the lower sensitivity of the high-temperature FIR experiment. The absence of any other phonon anomalies at higher frequencies does not support the existence of some phase transition near 200 K.

Interesting phonon anomalies are seen near 600 K (see Fig. 3). Some mode frequencies show relatively large temperature changes and splitting of the modes near 490 and 550 cm^{-1} that almost disappears above 600 K. However, it is important to stress that no mode from the doublet disappears above 600 K. Both modes remain in the spectra with similar frequencies near 520 cm^{-1} up to 900 K. Suchomel *et al.*[9] observed decomposition of BFCO ceramics on heating above 400 °C. This effect could also be responsible for the phonon anomalies seen near 600 K in our film, but we have to emphasize that we did not observe any decomposition in our sample (placed in a vacuum chamber of the spectrometer) because the IR spectra and magnetic properties (see below) were reproducible before and after the thermal cycling.

Phonon anomalies near T_N=640 K, similar to ours in Fig. 3, were observed in Raman spectra of BiFeO$_3$,[24,25] and they were explained by spin-phonon coupling. We will discuss

TABLE I. Factor group analysis of the optic lattice vibrations obtained in different (mostly hypothetical) crystal structures of Bi$_2$FeCrO$_6$. Note that only $R3$ and $C2/m$ phases were confirmed experimentally (Ref. 9). Activities of the phonons in IR and Raman spectra are marked in brackets. x,y,z means that the modes are active in IR spectra with electric vector $\mathbf{E}$ parallel to crystallographic axis x,y,z spectra, respectively. z^2, xy, etc., show components of Raman tensors, in which the phonons are Raman active. $E_g(R)$ means $E_g(x^2+y^2-2z^2, \sqrt{3}x^2-\sqrt{3}y^2)$.

$R3$-C_3^4	$C2/m$-C_{2h}^3	$P2mm$-C_{2v}^1	$I4/mcm$-D_{4h}^{18}	$Fm\bar{3}m$
$9A(z,x^2+y^2,z^2)$	$6A_u(z)$	$10A_1(z,x^2)$	$4A_{2u}(z)$	$4F_{1u}(x)$
$9E(x,y,x^2-y^2,xy,xz,yz)$	$12B_u(x,y)$	$7B_1(x,xz)$	$6E_u(x,y)$	
		$6B_2(y,yz)$	$2B_{2u}(-)$	$2F_{2g}(xy,yz,xz)$
	$5A_g(x^2,y^2,z^2,xy)$	$4A_2(xy)$	$2A_{1g}(x^2+y^2,z^2)$	$1A_{1g}(x^2+y^2+z^2)$
	$4B_g(xz,yz)$		$B_{1g}(x^2-y^2)$	$1E_g(R)$
			$2B_{2g}(xy)$	
			$2E_g(xz,yz)$	

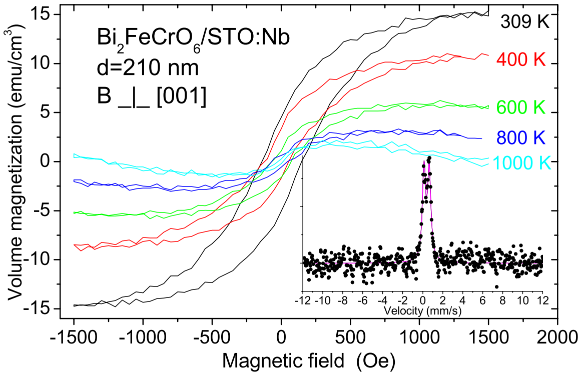

FIG. 4. (Color online) Magnetic hysteresis loops of BFCO thin partially B-site-ordered film deposited on STO:Nb substrate measured at selected temperatures up to 1000 K with magnetic field oriented perpendicular to the c axis of the thin film. Inset shows the room-temperature CEMS Mössbauer spectrum of the same film together with its fit.

this possibility below together with the magnetic data.

The phonon frequency changes seen near 600 K can be a consequence of some phase transition, but probably not a ferroelectric one because we see a gradual increase of the static permittivity $\varepsilon'(0)$ (from phonon contributions) on heating (see inset in Fig. 2), while for a ferroelectric transition, a maximum in $\varepsilon'(T)$ should be seen near T_c. If the high-temperature phase would be orthorhombic $P2mm$, we should see an enhanced number of modes (23 in total). In paraelectric tetragonal phase $I4/mcm$, ten modes are expected. If we assume that in our oriented film we see only modes active in $\mathbf{E}\|x,y$, spectra (i.e., E symmetry modes in the $R3$ phase), then we should see an enhanced number of modes in monoclinic (12) or orthorhombic (13) phases, but only 6 or 4 modes in tetragonal or cubic phase, respectively. We do not see any change of number of IR active modes above room temperature, so it seems that the ferroelectric phase transition in BFCO lies above 900 K, like for $BiFeO_3$. Further investigations, such as high-temperature structural or second harmonic generation, are needed for revealing the T_c and symmetry of the high-temperature phase(s).

Let us discuss the magnetic properties of BFCO thin film, which we investigated by means of vibration magnetometry and CEMS Mössbauer spectroscopy. The BFCO film (thickness of 600 nm) deposited on the $LaAlO_3$ substrate, originally investigated by IR spectroscopy, exhibits a strong diamagnetic signal from the substrate and the magnetic hysteresis loops were only revealed at low temperatures below 20 K (not shown here). It can be explained by a weak B-site order which suppresses the magnetic phase transition temperature.

On the other hand, the well-ordered BFCO thin film on the STO:Nb substrate exhibits nice magnetic hysteresis loops not only at RT but also at higher temperatures (see Fig. 4). Negative slope of magnetization at higher magnetic fields seen above 800 K can be explained by a diamagnetic contribution of the STO:Nb substrate, but below 600 K, the open hysteresis loop is clearly seen. The value of saturated magnetization is typical for antiferromagnets with weak ferromagnetism induced by a canted spin structure and the value of RT spontaneous magnetization corresponds well to the previously published results obtained on BFCO films.[4,5,10] Note that the magnetization is also comparable to values obtained on thick $BiFeO_3$ films.[26] The low value ($\sim 0.3\ \mu_B/\text{f.u.}$) of magnetization at saturation of the film regarding the expected theoretical value of $2\ \mu_B/\text{f.u.}$ (Ref. 3) could be explained by (i) the Fe-Cr ordering which may be only partial, (ii) the partial chemical disorder that generates an antiferromagnetic antisite contribution (Fe-Fe, Cr-Cr), and/or (iii) the partial relaxation of the strain in the film leading to a more distorted structure. It is not clear how large the contribution is of Fe and/or Cr ions to the measured spontaneous magnetization.

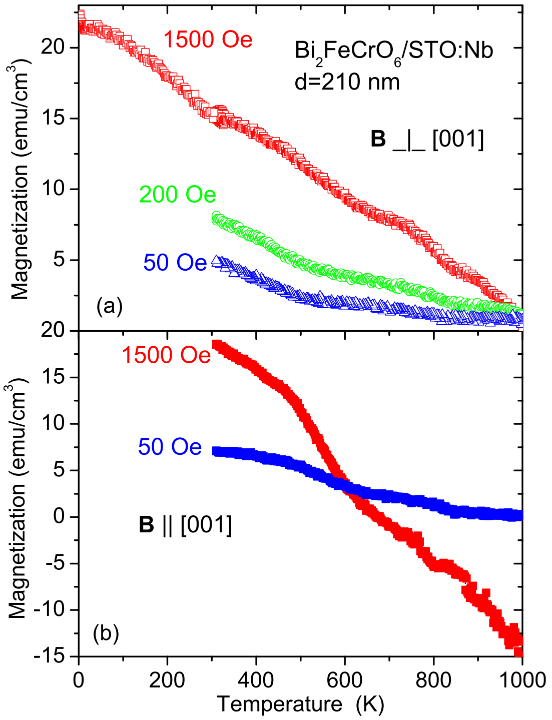

FIG. 5. (Color online) Temperature dependence of the magnetization in BFCO/STO:Nb film at various magnetic fields taken (a) perpendicular and (b) parallel to the c axis of the thin film.

Figure 5 shows the temperature dependence of the magnetization at various magnetic fields taken for two orientations of magnetic field—parallel and perpendicular to the (001) thin film plane, i.e., perpendicular and parallel to the [001] crystallographic direction of the thin film. At room temperature, one can see ≈30% higher magnetization in the [001] direction than that in the perpendicular orientation, but above 600 K, a diamagnetic signal from the substrate overcomes the magnetization from the thin film; therefore, the total measured magnetization becomes negative in the $\mathbf{B}\|[001]$ orientation. The magnetic anisotropy observed in BFCO thin films could be related to crystal anisotropy. The crystal structure analysis revealed that the Fe-O-Cr bond angle is slightly larger parallel to the c axis than that in the a-b plane. In all cases, the angles are less than 180°, which dramatically decrease the exchange integral and thus the magnetic properties and tends to favor an antiferromagnetic order for angles below 160°.

The magnetic experiments above and below 300 K were performed separately, which is probably the reason for the change of slope seen at 300 K in temperature dependence of magnetization measured at 1500 Oe. The magnetization remains nonzero up to 1000 K in the field of 1500 Oe, but the hysteresis loop is very slim at temperatures above 800 K. It is difficult to determine exactly the magnetic phase transition from Figs. 4 and 5, but it seems that it could lie somewhere between 600 and 800 K.

By means of vibration magnetometry, we investigated several thin films of BFCO deposited on STO:Nb. Their thicknesses ranged from 60 to 80 nm and the *B*-site order in these thin films was higher than that in the 210 nm film. The room-temperature magnetization of these films was comparable to the 210 nm film, but the measuring signal was lower due to the small thickness of the film; therefore, magnetization curves were noisier at high temperatures. For this reason, we do not present here the results obtained on thinner films. In the future, we plan experiments with a superconducting quantum interference device magnetometer, which is more sensitive and therefore will give more reliable results.

It is worth noting that Beattig *et al.*[8] predicted T_N in BFCO near 100 K, which corresponds to recent results of Suchomel *et al.*,[9] who claimed, based on transmission Mössbauer spectrum of BFCO ceramics, that T_N lies below 130 K. The low T_N of Suchomel *et al.* can be explained by chemical disorder in the Fe and Cr cations in the [111] direction,[9] while our thin film is at least partially chemically ordered (we observed satellite peaks both in the XRD and in the selected area electron diffraction patterns taken by TEM—see, e.g., Ref. 10).

The inset of Fig. 4 shows the room-temperature CEMS Mössbauer spectrum of the BFCO film. Surprisingly, only a doublet is seen, which is typical for the *paramagnetic* state of Fe^{3+} ions in the sample, while a sextet is expected in a magnetically ordered state. This is rather puzzling because clear magnetic hysteresis loops are seen in the same sample by vibration magnetometry (Fig. 4). Conversion electron Mössbauer spectroscopy of ^{57}Fe is based on the detection of electrons with the energy of 7.3 keV, which were knocked out of the *K* shell of the ^{57}Fe atom after re-emission of the gamma quantum originally resonantly absorbed by the ^{57}Fe nucleus. The release is almost instantaneous (within 10^{-7} s) and has a rather high probability. Most of these electrons are again absorbed in the material, but some of them, depending on the depth, where the electron emission occurs and on the electron work function, reach the surface of the sample and are finally detected. The depth from which the information is collected by the CEMS method is usually ∼200 nm depending on the absorption properties of the material; the electrons emitted from deeper regions of the sample do not reach the surface. Our thin film is only 210 nm thick, which means that we should see the CEMS signal from the whole volume of the film. However, the film is not only magnetic but also ferroelectric, and electric field in the ferroelectric domains may substantially influence the work function of the electrons. The ferroelectric domain structure of BFCO is complex and assuming that it is similar to that reported for $BiFeO_3$,[27] the polarization (and related internal electric field) is oriented 41.8° or even 131.8° to the normal surface of the (001)-oriented thin film. Therefore, the emitted electrons are returned back to the film and most of them lose their energy, are absorbed, and do not leave the film. Only electrons emitted from a very thin surface layer (∼10 nm) may reach the surface and are detected in the CEMS experiment. The thin film surface layer is most likely nonmagnetic (probably due to chemical disorder of Fe and Cr cations at the surface); therefore, only a doublet is observed in our CEMS Mössbauer spectra shown in the inset of Fig. 4, although the volume of the film is magnetically ordered, as clearly seen from the magnetic hysteresis loops measured by vibrating-sample magnetometry.

TABLE II. Comparison of the fit parameters of Mössbauer spectra in Fig. 4 and in Ref. 9.

	Our data (CEMS)	Suchomel *et al.*[a] (Trans. mode)
Isomer shift δ (mm/s)	0.39	0.39
Quadrupole splitting ΔE_q (mm/s)	0.52	0.48
"Peak width"—FWHM (Γ) (mm/s)	0.39	N/A

[a]Reference 9.

The doublet in CEMS spectrum of magnetic BFCO film could also be theoretically explained by the hypothesis that the magnetization of the film comes only from Cr^{3+} ions and Fe^{3+} ions are in a paramagnetic state. However, such explanation is not likely, although it cannot be excluded.

We have to stress that we repeated the CEMS Mössbauer experiment also with another 86 nm thick BFCO film deposited on STO:Nb substrate, which exhibited strong satellites in the XRD (i.e., a higher Fe and Cr chemical order than that in the previous sample), as well as broad magnetic hysteresis loops, and we still found only a doublet in CEMS spectra typical for the paramagnetic order. Finally, we note that the doublet cannot originate from the substrate because the Mössbauer spectrum is only due to the Fe nuclei not present in the STO:Nb substrate.

Parameters of the Mössbauer spectra fit are summarized in Table II. From the Fe isomer shift δ, the valency of the iron can be clearly estimated. The Fe^{3+} cations in the oxidic compound have their isomer shifts in the range of 0.1–0.5 mm/s, while the Fe^{2+} cations show δ in the range of 0.8–1.5 mm/s.[28] Our obtained value $\delta=0.39$ mm/s confirms the absence of Fe^{2+} states and the presence of only Fe^{3+} states in the investigated film. Mössbauer spectra also allow us to determine the site symmetry for Fe^{3+} cations in the structure. According to Refs. 28 and 29, the usual isomer shift values for Fe^{3+} in the case of the spectra measured at RT are as follows: 0.10–0.30 mm/s for Fe^{3+} in a tetrahedral site and 0.28–0.50 mm/s for Fe^{3+} in an octahedral site. When we compare the above-mentioned ranges with our $\delta=0.39$ mm/s, we can confirm that Fe^{3+} in BFCO is in the octahedral position.

When we compare our fitting parameters in Table II with the parameters obtained from the Mössbauer spectra (measured in the transmission mode) of disordered ceramics published by Suchomel *et al.*,[9] we can state that both ceramics and surface layer of our thin film have the same or similar nonmagnetic structure at RT, although the magnetic measurements by vibrating-sample magnetometry give evidence for a magnetic order inside the thin film far above RT.

In light of our high-temperature magnetic data, we can suggest that the phonon anomalies seen near 600 K are due to a magnetic phase transition. Near this temperature, a sudden drop of the permittivity is seen, which is typical for spin-phonon coupling.[30] Nevertheless, further magnetic, structural, and dielectric studies are necessary for the confirmation of this hypothesis.

IV. CONCLUSION

The high-frequency complex dielectric response of a BFCO film was determined by IR reflectance of a BFCO thin film deposited on a $LaAlO_3$ substrate. Most of the polar phonons seen in the IR spectra reveal gradual softening on heating from 20 to 900 K, which causes a progressive increase of the static permittivity with increasing temperature. Therefore, we speculate that the ferroelectric phase transition lies (similarly to the related $BiFeO_3$) above 900 K, although some phonon anomalies, probably connected with a magnetic phase transition, were observed near 600 K. Magnetic properties of BFCO thin films deposited on STO:Nb substrate were investigated between 6 and 1000 K and revealed that the BFCO films are good high-temperature multiferroics with a magnetic phase transition between 600 and 800 K. Conversion electron Mössbauer spectrum did not reveal magnetic order in the BFCO thin film in contrast to vibration magnetometry because the electric field presented in ferroelectric domains extends the track of emitted electrons and prevents their detection from most of the volume depth of the thin film. Therefore, the collected electrons are probably only from a thin nonmagnetic surface layer of the film. Further structural, magnetic, and dielectric high-temperature studies on well *B*-site-ordered samples are in progress.

ACKNOWLEDGMENTS

The work was supported by the Grant Agency of the Czech Republic (Project No. 202/06/0403) and Grant Agency of Academy of Science of the Czech Republic (Projects No. KJB100100704 and No. AVOZ10100520. Part of this research was supported by grants from the Natural Sciences and Engineering Research Council of Canada (NSERC) as well as from the Fond Québécois de la Recherche sur la Nature et les Technologies (FQRNT). The authors thank J. Šebek for valuable discussions as well as J. Petzelt and T. W. Johnston for critical reading of the manuscript.

---

*kamba@fzu.cz

[1] M. Fiebig, J. Phys. D **38**, R123 (2005).
[2] S.-W. Cheong and M. Mostovoy, Nat. Mater. **6**, 13 (2007).
[3] P. Baettig and N. A. Spaldin, Appl. Phys. Lett. **86**, 012505 (2005).
[4] R. Nechache, C. Harnagea, A. Pignolet, F. Normandin, T. Veres, L.-P. Carrignan, and D. Ménard, Appl. Phys. Lett. **89**, 102902 (2006).
[5] R. Nechache, C. Harnagea, L.-P. Carrignan, D. Ménard, and A. Pignolet, Philos. Mag. Lett. **87**, 231 (2007).
[6] D. H. Kim, H. N. Lee, M. D. Biegalski, and H. M. Schristen, Appl. Phys. Lett. **91**, 042906 (2007).
[7] M. Alexe and L. Pintilie (private communication).
[8] P. Baettig, C. Ederer, and N. A. Spaldin, Phys. Rev. B **72**, 214105 (2005).
[9] M. R. Suchomel, Ch. I. Thomas, M. Allix, M. J. Rosseinsky, A. M. Fogg, and M. F. Thomas, Appl. Phys. Lett. **90**, 112909 (2007).
[10] R. Nechache, L.-P. Carignan, L. Gunawan, C. Harnagea, G. A. Botton, D. Ménard, and A. Pignolet, J. Mater. Res. **22**, 2102 (2007).
[11] S. Kamba, M. Kempa, V. Bovtun, J. Petzelt, K. Brinkman, and N. Setter, J. Phys.: Condens. Matter **17**, 3965 (2005).
[12] B. G. Almeida, A. Pietka, P. Caldelas, J. A. Mendes, and J. L. Ribeiro, Thin Solid Films **513**, 275 (2006).
[13] T. Yamada, J. Petzelt, A. K. Tagantsev, S. Denisov, D. Noujni, P. K. Petrov, A. Mackova, K. Fujito, T. Kiguchi, K. Shinozaki, N. Mizutani, V. O. Sherman, P. Muralt, and N. Setter, Phys. Rev. Lett. **96**, 157602 (2006).
[14] K. A. Müller, W. Berlinger, and F. Waldner, Phys. Rev. Lett. **21**, 814 (1968).
[15] F. Gervais, in *Infrared and Millimeter Waves*, edited by K. J. Button (Academic, New York, 1983), Vol. 8, Chap. 7, p. 279.
[16] M. Born and E. Wolf, *Principles of Optics* (Pergamon, Oxford, 1960).
[17] O. S. Heavens, Rep. Prog. Phys. **22**, 1 (1960).
[18] D. L. Rousseau, R. P. Bauman, and S. P. S. Porto, J. Raman Spectrosc. **10**, 253 (1981).
[19] R. Palai, R. S. Katiyar, H. Schmid, P. Tissot, S. J. Clark, J. Robertson, S. A. T. Redfern, G. Catalan, and J. F. Scott, Phys. Rev. B **77**, 014110 (2008).
[20] I. A. Kornev, S. Lisenkov, R. Haumont, B. Dkhil, and L. Bellaiche, Phys. Rev. Lett. **99**, 227602 (2007).
[21] S. Kamba, D. Nuzhnyy, M. Savinov, J. Sebek, J. Petzelt, J. Prokleska, R. Haumont, and J. Kreisel, Phys. Rev. B **75**, 024403 (2007).
[22] P. Hermet, M. Goffinet, J. Kreisel, and Ph. Ghosez, Phys. Rev. B **75**, 220102(R) (2007).
[23] R. P. S. M. Lobo, R. L. Moreira, D. Lebeugle, and D. Colson, Phys. Rev. B **76**, 172105 (2007).
[24] R. Haumont, J. Kreisel, P. Bouvier, and F. Hippert, Phys. Rev. B **73**, 132101 (2006).
[25] H. Fukumura, S. Matsui, H. Harima, T. Takahashi, T. Itoh, K. Kisoda, M. Tamada, Y. Noguchi, and M. Miyayama, J. Phys.: Condens. Matter **19**, 365224 (2007).
[26] J. Wang, A. Scholl, H. Zheng, S. B. Ogale, D. Viehland, and D. G. Schlom, Science **307**, 1203b (2005).
[27] Y.-H. Chu, L. W. Martin, M. B. Holcomb, and R. Ramesh, Mater. Today **10**, 16 (2007).
[28] F. Menil, J. Phys. Chem. Solids **46**, 763 (1985).
[29] J. Parmentier, S. Vilminot, and J.-L. Dormann, Solid State Sci. **1**, 257 (1999).
[30] G. A. Smolenskii and I. Chupis, Sov. Phys. Usp. **25**, 475 (1982).